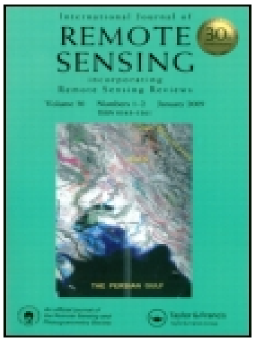

Taylor & Francis
Taylor & Francis Group

International Journal of Remote Sensing

ISSN: 0143-1161 (Print) 1366-5901 (Online) Journal homepage: http://www.tandfonline.com/loi/tres20

Quantifying livestock effects on bunchgrass vegetation with Landsat ETM+ data across a single growing season

Vincent S. Jansen, Crystal A. Kolden, Robert V. Taylor & Beth A. Newingham

To cite this article: Vincent S. Jansen, Crystal A. Kolden, Robert V. Taylor & Beth A. Newingham (2016) Quantifying livestock effects on bunchgrass vegetation with Landsat ETM+ data across a single growing season, International Journal of Remote Sensing, 37:1, 150-175, DOI: 10.1080/01431161.2015.1117681

To link to this article: http://dx.doi.org/10.1080/01431161.2015.1117681

INTERNATIONAL JOURNAL OF REMOTE SENSING, 2015
VOL. 37, NO. 1, 150–175
http://dx.doi.org/10.1080/01431161.2015.1117681

Quantifying livestock effects on bunchgrass vegetation with Landsat ETM+ data across a single growing season

Vincent S. Jansen[a,b], Crystal A. Kolden[b], Robert V. Taylor[c] and Beth A. Newingham[d]

[a]Environmental Science Department, University of Idaho, Moscow, ID, USA; [b]Department of Geography, University of Idaho, Moscow, ID, USA; [c]The Nature Conservancy, Enterprise, OR, USA; [d]Department of Forest, Rangeland, and Fire Sciences, University of Idaho, Moscow, ID, USA

ABSTRACT

Grassland systems provide important habitat for native biodiversity and forage for livestock, with livestock grazing playing an important role influencing sustainable ecosystem function. Traditional field techniques to monitor the effects of grazing on vegetation are costly and limited to small spatial scales. Remote sensing has the potential to provide quantitative and repeatable monitoring data across large spatial and temporal scales for more informed grazing management. To investigate the ability of vegetation metrics derived from remotely sensed imagery to detect the effect of cattle grazing on bunchgrass grassland vegetation across a growing season, we sampled 32 sites across four prescribed stocking rates on a section of Pacific Northwest bunchgrass prairie in northeastern Oregon. We collected vegetation data on vertical structure, biomass, and cover at three different time periods: June, August, and October 2012 to understand the potential to measure vegetation at different phenological stages across a growing season. We acquired remotely sensed Landsat Enhanced Thematic Mapper Plus (ETM+) data closest in date to three field sampling bouts. We correlated the field vegetation metrics to Landsat spectral bands, 14 commonly used vegetation indices, and the tasselled cap wetness, brightness, and greenness transformations. To increase the explanatory value of the satellite-derived data, full, stepwise, and best-subset multiple regression models were fit to each of the vegetation metrics at the three different times of the year. Predicted vegetation metrics were then mapped across the study area. Field-based results indicated that as the stocking rate increased, the mean vegetation amounts of vertical structure, cover, and biomass decreased. The multiple regression models using common vegetation indices had the ability to discern different levels of grazing across the study area, but different spectral indices proved to be the best predictors of vegetation metrics for differing phenological windows. Field measures of vegetation cover yielded the highest correlations to remotely sensed data across all sampling periods. Our results from this analysis can be used to improve grassland monitoring by providing multiple measures of vegetation amounts across a growing season that better align with land management decision making.

ARTICLE HISTORY
Received 19 March 2015
Accepted 28 October 2015

CONTACT Vincent S. Jansen jans4886@vandals.uidaho.edu

1. Introduction

The world's temperate grassland ecosystems are of high conservation importance, as nearly half the historic area has been converted to different land-use types and less than 5% of what remains falls under conservation protection (Henwood 2010; Hoekstra et al. 2005). Grasslands provide important ecosystem services (Svoray, Perevolotsky, and Atkinson 2013), including forage for the livestock industry and vital habitat for native wildlife (Chapin et al. 1996; Conner et al. 2002). Due to the potential adverse effects that grazing poses to structure and function of grasslands (Johnson et al. 2011; Milchunas and Lauenroth 1993), their value for wildlife (Johnson, Kennedy, and Etterson 2012; Kimoto et al. 2012), and the economic viability of ranching enterprises (Holechek et al. 1999), cost-effective monitoring techniques are needed that are able to identify trends, thresholds, and tipping points for sustainable grazing management and grassland ecosystem services (Smith et al. 2014). Accurate, cost-effective monitoring that is quantitative and repeatable across large spatial extents has proven to be difficult with traditional, field-based rangeland monitoring techniques (Booth and Tueller 2003; Pickup, Bastin, and Chewings 1994; Washington-Allen et al. 2006; West 2003). Therefore timely monitoring of heterogeneous vegetation across large areas requires new methods and technology (Hunt, et al. 2003; Pickup, Bastin, and Chewings 1994). The relatively recent focus on acquiring scalable, quantitative data for decision support has led to remote sensing as a way to improve existing monitoring data sets (Herrick et al. 2010). While some progress has been made in deriving empirical, repeatable measures of important grassland vegetation metrics from remote sensing (Hagen et al. 2012; Marsett et al. 2006; Todd, Hoffer, and Milchunas 1998), challenges remain to provide accurate measures of multiple vegetation metrics over large grassland areas across growing seasons. Development of scalable, season-specific metrics is critical for improved understanding of drivers of rangeland condition, and to the decision-support needs of rangeland managers tasked with implementing sustainable grazing management programmes.

Space-borne remote-sensing data have the potential to provide repeatable vegetation monitoring data at management-relevant spatial scales (Hagen et al. 2012; Tsalyuk et al. 2015). Previous investigations used a variety of analysis techniques to quantify common rangeland monitoring metrics, such as vertical structure (Marsett et al. 2006), cover (Blanco, Ferrando, and Biurrun 2009; Hagen et al. 2012; Purevdorj et al. 1998; Röder et al. 2008; Marsett et al. 2006), and biomass (Brinkmann et al. 2011; Schino et al. 2003; Todd, Hoffer, and Milchunas 1998; Marsett et al. 2006). Field measures are typically correlated to vegetation indices or transformations derived from remotely sensed data (Dungan 1998) to determine the most applicable spectral index for vegetation monitoring (Zhang and Guo 2008). Data for these relationships are derived from field data collected at training sites and satellite-derived data from the geospatially co-located pixel or pixel window corresponding to that site (Dungan 1998; Marsett et al. 2006; Vescovo and Gianelle 2008; Yang and Guo 2011; Zhang and Guo 2008). Once relationships are established between vegetation field metrics and remotely sensed data, grazing effects have been quantified in a variety of ways (Kawamura et al. 2005; Pickup, Bastin, and Chewings 1998; Yang and Guo 2011). Methods used include testing the relationship between stocking rates and remotely sensed vegetation data (Numata et al. 2007) or comparing the average vegetation index values between pasture areas with different grazing intensities (Yang and Guo 2011). Grazing management practices have also been assessed by quantifying the trend in a specific vegetation index across many years (Archer 2004; Bradley and O'sullivan 2011; Evans and Geerken 2004; Hill et al. 1998; Röder et al. 2008; Washington-Allen et al. 2006; Yang, Guo, and Fitzsimmons 2012), or establishing a grazing gradient to quantify how vegetation cover changes with distance from a water source for livestock (Lind et al. 2003; Pickup, Bastin, and Chewings 1994, 1998).

Although these approaches provide some understanding of the change in vegetation amounts caused by grazing, remotely sensed products for rangeland management decision making are still lacking (Butterfield and Malmstrom 2006; Hagen et al. 2012; Hunt, Jr. et al. 2003; Marsett et al. 2006; Washington-Allen et al. 2006). Specifically, rangeland management decision making occurs across the span of a season to a full year, but most prior studies have primarily quantified vegetation during a narrow window of peak greenness (e.g. Brinkmann et al. 2011; Paudel and Andersen 2010). In many grassland systems, pastures continue to be grazed after peak greenness, impacting vegetation quantities and the metrics utilized by land managers to plan grazing for the following year (Hagen et al. 2012; Marsett et al. 2006). Rangeland managers need timely, in-season information regarding vegetation quantities and livestock impacts during the grazing season for adaptive decision making (Anderson and Currier 1973; Tueller 1989), as well as end-of-year measures (i.e. not peak greenness) to make decisions regarding stocking rate, timing, and pasture rotations for the near future (Holechek 1988; Tsalyuk et al. 2015).

Creating remote-sensing products that align with vegetation measures across the yearly grazing management cycle or growing season can increase the utility of remotely sensed data for management decision making. Providing such data, however, depends on the ability of remote-sensing data to quantify vegetation amounts at different phenological stages (i.e. actively growing or senescent vegetation). Typical greenness indices, such as the normalized difference vegetation index (NDVI), have been correlated to many vegetation measures such as cover, biomass, and leaf area index (LAI) during vegetation photosynthesis, but lose accuracy as the vegetation senesces or turns brown (Butterfield and Malmström 2009; Hagen et al. 2012; Marsett et al. 2006; Numata et al. 2007; Schino et al. 2003). Vegetation senescence across the growing season creates the need to explore multiple vegetation indices to measure vegetation amounts at various time periods across the year (Hagen et al. 2012; Marsett et al. 2006; Numata et al. 2007). In an ideal decision-support framework, land managers could track common rangeland vegetation monitoring metrics across the growing season (Hagen et al. 2012; Marsett et al. 2006) and monitor changes in these metrics with different stocking rates to make more informed decisions for both current and ensuing grazing periods.

The Pacific Northwest bunchgrass prairie is a unique grassland habitat that is sensitive to grazing pressure (Johnson et al. 2011; McLean and Tisdale 1972; Skovlin et al. 1976). Like many grassland systems that experience a summer dry season, grazing on this grassland type predominantly occurs in the summer and fall months (Bartuszevige, Kennedy, and Taylor 2012), mostly after peak greenness. Thus, to monitor grazing impacts in this region requires a remote-sensing approach that spans the growing season. Only a few studies have tried to quantify vegetation response to various grazing intensities (Munyati and Makgale 2009; Numata et al. 2007; Yang and Guo 2011), and even fewer have tested the utility of multiple spectral indices to track grazing impacts over the course of a single growing season (Hagen et al. 2012).

The primary objective of this study was to develop seasonal models of rangeland condition from remotely sensed data. Specifically, we assessed relationships between field measurements and spectral indices over a growing season to identify the best spectral predictors of grazing effects on multiple common rangeland metrics, and determined whether these predictors provide (1) reliable estimation of vegetation amounts over time at different points in the grazing season, and (2) measures which are sensitive to various stocking rates. We assessed the relationship of moderate-resolution Landsat data to three vegetation metrics (i.e. vegetation cover, biomass, and vertical structure) measured during three different temporal periods across four stocking rates on a semi-arid bunchgrass prairie in northeastern Oregon. To determine spectral sensitivity, we (1) characterized relationships between field-based metrics and grazing intensities, (2) quantified relationships between Landsat data and field-based metrics, and (3) assessed the strength of the spectral relationships across the growing season. We hypothesized that if significant relationships between spectral indices and vegetation metrics remained consistent across the growing season and grazing levels, one could evaluate how vegetation amounts differed across the landscape and between stocking rates, thereby providing management data to help guide more informed and sustainable grazing rotations.

2. Methods

2.1. *Study area*

The study was conducted in 2012 on the Zumwalt Prairie Preserve, owned by The Nature Conservancy (TNC) (45°33′ N, 117°02′ W, elevation 1500 m) in Wallowa County, Oregon, USA (Figure 1). The Zumwalt Prairie Preserve (13,000 ha) constitutes a small portion of the larger Zumwalt Prairie grassland, which is approximately 130,000 ha in area. These grasslands are dominated by C_3 grasses that include Idaho fescue (*Festuca idahoensis* Elmer), bluebunch wheatgrass (*Pseudoroegneria spicata* (Pursh) A. Love), and Sandberg's

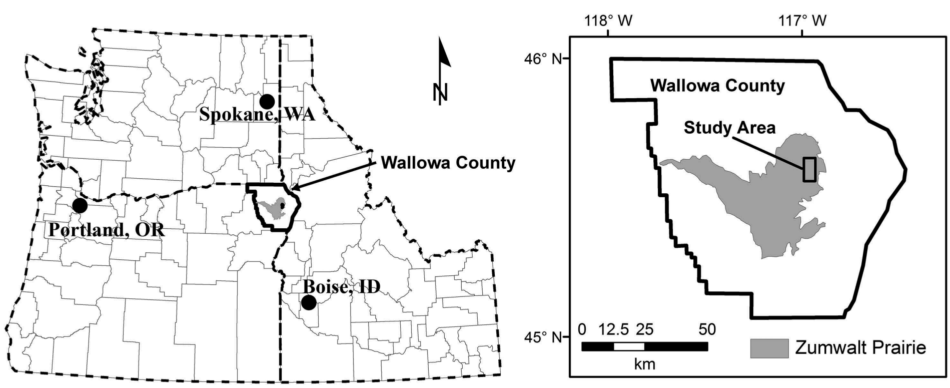

Figure 1. Map of the study area, Zumwalt Prairie, Oregon.

bluegrass (*Poa secunda* J Presl). Annual invasive grasses are relatively sparse across the study area, comprising less than 5% of the total vegetation (Oregon State University, unpublished data). Average summer (June–August) temperatures range from 11.8 to 17.5°C, with an average annual precipitation of 348 mm (2006–2012 Zumwalt Weather Station), although most of this falls outside of the summer season. The growing season on the prairie typically begins in April and ends in October. Although many grassland systems worldwide are now used for crop production, the Zumwalt Prairie was not converted to cultivation due to the short growing season and mostly shallow soils (Bartuszevige, Kennedy, and Taylor 2012). Before the area was settled by Anglo-Americans, the Nez Perce Tribe (Nimíipuu) grazed horses and cattle beginning in the 1700s (Bartuszevige, Kennedy, and Taylor 2012). The majority of land currently on the Zumwalt Prairie is privately owned and livestock grazing has been the major land use for over a century, with spring/summer pasturing of beef cattle the predominant use in the last half century (Bartuszevige, Kennedy, and Taylor 2012).

2.2. *Study design*

To define the suitable habitat sampling area, we limited our study to the ecological systems 'Columbia Basin Palouse Prairie' and 'Columbia Basin Foothill and Canyon Dry Grassland' as defined by the ReGap Ecological Systems data (Kagan et al. 2006). To reduce spectral noise from path radiance and shadowing of slopes, the analysis area was limited to sites of less than 30% slope and at least 50 m away from roads, stock ponds, and fence lines, and at least 200 m from other field sites.

Grazing treatment levels (stocking rates) were prescribed by TNC land managers to align with prior grazing studies on the Zumwalt Prairie (Johnson et al. 2011). The pastures were stocked with cattle at four different animal unit months (AUM) per hectare (AUM ha^{-1}). One AUM is the amount of forage consumed by an adult cow and her calf across a 30-day period. High grazing treatments were stocked at 1.08 AUM ha^{-1}, medium at 0.72 AUM ha^{-1}, and low at 0.36 AUM ha^{-1}. Control areas were not grazed by livestock (0.00 AUM ha^{-1}). Pastures ranged in size from 40 ha (C3 and D3 pastures) to 185 ha (far north). It is assumed, based upon prior vegetation research across the study area (Johnson et al. 2011), that site potential (i.e. vegetation amount) does not significantly differ between treatment areas. Field data were collected in three different sampling bouts: 26 June–4 July, 10–16 August, and 27 September–5 October, 2012, with peak greenness occurring just before the start of the first sampling bout (Figure 2). Thirty-two sites across three different stocking rates were sampled in each bout. We were unable to sample within the pastures with low stocking rates due to limited resources and time constraints (i.e. needing to collect field data within a limited window around a Landsat acquisition date and before significant changes in phenology occurred); we considered it was more critical to focus on sampling moderate and high stocking rate pastures. A geographical information system (GIS) was used to generate random sampling points, and when those points were reached in the field, the nearest homogenous area to the pre-identified point was sampled. Sample sites were chosen to best represent a gradient of vegetation amounts (Wylie et al. 2002). Twelve sampling sites were placed in pastures with a high stocking rate, 10 sites in pastures with a medium rate, and 10 in control (no-graze) pasture areas (Figure 2).

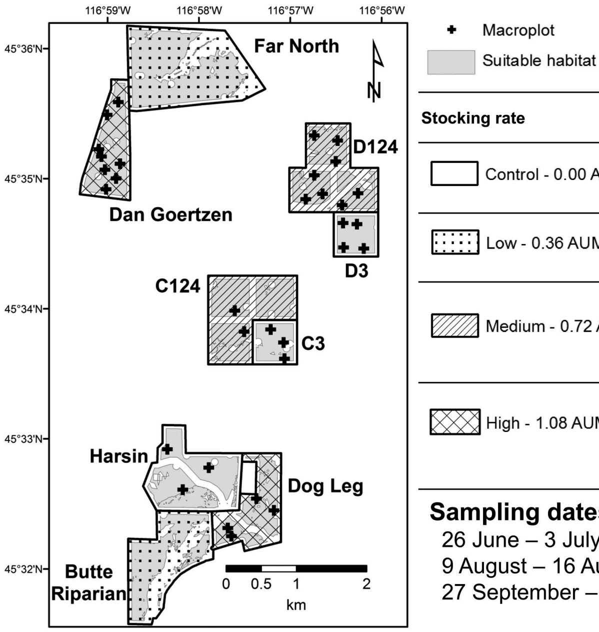

Stocking rate	Pastures	Size (ha)	Dates grazed	*N*
Control - 0.00 AUM/ha	C3, D3, Harsin,	40 40 120	No graze	10
Low - 0.36 AUM/ha	Far North, Butte Riparian	185 123	1 June – 23 June	0
Medium - 0.72 AUM/ha	C124	120	16 June – 4 August	10
	D124	120	31 May – 22 June	
High - 1.08 AUM/ha	Dan Goertzen	82	28 May – 21 June	12
	Dogleg	86	28 May – 11 June	

Sampling dates
26 June – 3 July
9 August – 16 August
27 September – 5 October

Figure 2. Grazing treatment map showing livestock stocking rates, timing of grazing, and the number (*N*) and location of macro-plots sampled within each pasture. Suitable habitat analysis area is delineated using two ecological systems 'Columbia Basin Palouse Prairie' and 'Columbia Basin Foothill and Canyon Dry Grassland' from ReGap (Kagan et al. 2006); and areas with less than 30% slope, at least 50 m away from roads, stock ponds, and fence lines.

2.3. *Biophysical vegetation measures*

Three vegetation metrics were sampled across the growing season to be modelled by remotely sensed data: vegetation structure, foliar cover, and biomass. At each sampling site a 30 m × 30 m macro-plot was established with two 30 m transects intersecting the plot centre aligned in north/south and east/west cardinal directions. Within each macro-plot, data on vegetation structure, foliar cover, and biomass were collected at three time periods during the grazing season. Vegetation structure data were collected every 5 m along each transect by measuring the lowest visible decimetre line on a Robel pole fixed perpendicular to the ground. From opposite cardinal directions, measurements were read off the pole from 4 m in distance and 1 m above ground height (Robel et al. 1970) along the two transects for a total of 13 measures per macro-plot. Foliar cover data were collected every metre on each transect using the line-point intercept method (Herrick et al. 2005). Biomass was measured by clipping all vegetation standing crop within two systematically random 0.5 m × 0.5 m quadrats located 15 m from each other per transect to 0.5 cm above ground surface (Table 1). The first quadrat location for each bout and transect had a random start location between 0 and 15 m generated (no start locations were duplicated between bouts), the second plot being systematically placed 15 m away along the same transect. To obtain dry weight, clipped vegetation was dried in an oven at 60°C for 24–36 hours until the weight remained stable. The final weight of each sample was averaged by macro-plot and used as the measure of dry biomass.

Table 1. Field metrics collected for each sampling bout across the growing season at each of the 32 macro-plots.

Sample bouts	Field metric	Method	Samples per site (N)
1,2,3	Foliar cover	Line-point intercept – Herrick et al. 2005	60
1,2,3	Biomass	Clip plots	4
1,2,3	Vegetation structure	Robel et al. 1970	13
3	Utilization	Parsons et al. 2003	10

2.4. *Utilization measure*

Grazing impacts can be assessed by measuring utilization at the end of the year to provide information on how much vegetation has been consumed or destroyed by livestock (Coulloudon et al. 1999). Utilization was visually estimated at each macro-plot during the last sampling bout in October, using the double-weight sampling method described by Parsons et al. (2003) (Table 1). The average utilization per macro-plot was computed by taking the average percent utilization estimated across 10 randomly placed 0.25 m × 0.25 m quadrats. To account for estimation bias, observers first estimated utilization amounts (0–100%) in fifteen 0.25 m × 0.25 m calibration quadrats, each of which had varying amounts of vegetation removed to mimic different utilization rates prior to sampling. After each observer-estimated utilization, the residual vegetation was clipped to within 0.5 cm of the ground and weighed. The initial clipped vegetation weight was then divided by the total weight (initial + final clipped weight) of the vegetation within the quadrat to obtain utilization (Parsons et al. 2003). For each observer, regression equations were constructed by regressing estimated utilization against actual utilization (e.g. Parsons et al. 2003). Observer 1's regression equation was $y = 0.711x + 12.07$, with a coefficient of determination (R^2) = 0.59 and $p = 0.001$; observer 2's regression was $y = 0.735x + 7.291$, with an $R^2 = 0.81$ and $p < 0.001$. These equations were then used to correct the observers' estimated utilization for each sample obtained at each macro-plot. Differences in utilization amounts between stocking rates were then computed using ANOVA. When a significant overall effect was found, t-tests between all possible treatment pairs were computed.

2.5. *Remotely sensed data*

The need to measure vegetation in a cost-effective manner and at different times outside of peak greenness, coupled with the spatial scales of grazing management decision making, determines the satellite platform to use for quantifying grazing impacts on vegetation. The two freely available and most widely-used sensors to measure grazing effects are Landsat and the Moderate Resolution Imaging Spectroradiometer (MODIS) (Hagen et al. 2012). One challenge with MODIS lies in the coarse spatial resolution (250–1000 m), which makes it difficult to accurately scale spectral data to field data (Hagen et al. 2012). By comparison, Landsat (at 30 m resolution) is more easily related to plot-level field data and provides a greater number of pixels for statistical analysis between distinct management areas. For these reasons, Landsat has been shown to be a well-suited sensor for rangeland management purposes (Ikeda, Okamoto, and Fukuhara 1999; Kurtz, Schellberg, and Braun 2010; Marsett et al. 2006; Röder et al. 2008; Xu and Guo 2015). Due to the spatial scales of management across the study area and the greater ability to accurately scale up from the field data, we selected Landsat data to quantify grazing impacts for this analysis.

We acquired 11 terrain-corrected (L1T) Landsat Enhanced Thematic Mapper Plus (ETM+) scenes from the middle of June to early October for 2012 from WRS-2 path/rows 42/28 and 43/28 using the USGS EarthExplorer website (http://earthexplorer.usgs.gov/). The Standard Terrain Corrected (L1T) product corrects for radiometric and geometric inaccuracies of Landsat data. Each Landsat ETM+ scene was processed to top-of-atmosphere reflectance using the ETM+ radiometric coefficients from Chander, Markham, and Helder (2009) and then atmospherically corrected to at-surface reflectance using the improved image-based cosine model (Chavez 1996). To relate the satellite data to field data, Landsat scenes closest in date to the three field sampling bouts were selected as base scenes. For pixels falling within 'no data' lines associated with the Landsat 7 scan line corrector malfunction or obscured by cloud cover, data were gap-filled with data from the next closest scene in date containing valid data within the same growing season. For the first sampling bout, the 3 July 2012 scene was used as the base scene, and pixels falling within areas of no data were gap-filled with scene data from either 17 June or 12 July 2012, producing a 7.56-day average (minimum = 1, maximum = 14 days) time difference between the plot sampling date and the closest valid satellite data scene date. For the second sampling bout, the 13 August 2012 scene was gap-filled with the 4 August 2012 data producing a 2.4-day average (minimum = 0, maximum = 10 days) between field and satellite data. For the third sampling bout, the 30 September 2012 scene was gap-filled with the 7 October 2012 scene with a 4.96 day average (minimum = 3, maximum = 12 days) between field and satellite data. Mean at-surface reflectance for each band was then computed across four pixels using a 2×2 pixel window average to fully cover each macro-plot. Band data and vegetation indices were then computed for each site using the averaged values for each band. From these reflectance data, vegetation indices and transformations were computed for each sample site for each sampling bout (Figure 3).

2.6. *Vegetation indices*

At-surface reflectance data from Landsat ETM+ bands 1–5 and 7, as well as 14 vegetation indices and the tasselled cap transformations (Kauth and Thomas 1976), were used to estimate relationships with biophysical vegetation data (Table 2). Vegetation indices calculated were the simple ratio (SR; Jordan 1969), NDVI (Rouse et al. 1973; Tucker 1979), soil adjusted vegetation index (SAVI; Huete 1988), renormalized difference vegetation index (RDVI; Haboudane et al. 2004; Roujean and Breon 1995), modified triangular vegetation index 1 (MTVI1; Haboudane et al. 2004), canopy index (CI; Vescovo and Gianelle 2008), normalized canopy index (NCI; Vescovo and Gianelle 2008), ratio cover index (RCI; Zhang and Guo 2008), normalized difference cover index (NDCI; Zhang and Guo 2008), plant senesce reflectance index (PSRI; Merzlyak et al. 1999), soil adjusted total vegetation index (SATVI; Marsett et al. 2006), the seven/four ratio (7/4), normalized difference infrared index seven (NDII7; Hardisky, Smart, and Klemas 1983; Key and Benson 2006), normalized difference water index (NDWI; Hardisky, Smart, and Klemas 1983; Gao

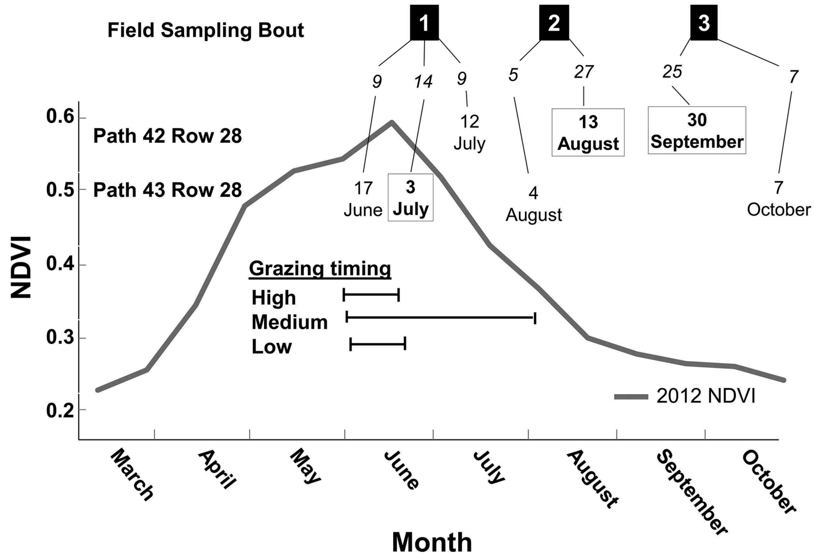

Figure 3. Timing of the three sampling bouts (the numbered black boxes) in relation to Landsat ETM+ scenes used in the analysis process shown as dates in 2012. Scene data used to build relationships to field sampling bout data are connected by lines, with base scenes outlined by boxes. The number on each line represents the number of macro-plots corresponding to that scene date. The timing of livestock grazing grouped by stocking rate is represented by black lines. The normalized difference vegetation index (NDVI) is represented by the grey line; these data are from the 16-day NDVI MODIS product (ORNL DAAC 2012).

1996), and the tasselled cap transformations (Kauth and Thomas 1976) greenness (TCGRE), brightness (TCBRI), and wetness (TCWET) from reflectance data (Crist 1985) (Table 2).

These vegetation indices were selected based on prior research performed on other grasslands (e.g. Marsett et al. 2006; Numata et al. 2007; Yang and Guo 2011; Zhang and Guo 2008). Vegetation indices that incorporate red (band 3) and near-infrared (NIR; band 4) bands have been shown to be effective in measuring green vegetation amounts by differencing the reflectance values between the near-infrared and red portion of the electromagnetic spectrum (Marsett et al. 2006; Rouse et al. 1973; Tucker 1979). Indices that incorporate the shortwave infrared bands [bands 5 (SWIR1) and 7 (SWIR2)], which are sensitive to water content, provide good measurements of both green and senescent vegetation quantity (Hardisky, Smart, and Klemas 1983; Marsett et al. 2006; Numata et al. 2007; Pickup, Bastin, and Chewings 1994; Yang and Guo 2011). Vegetation indices that incorporate SWIR band 7 in combination with the NIR band are typically used for forest disturbances, such as fire, and can be used to differentiate live vegetation from soil, ash, and dead vegetation (Key 2006). The tasselled cap transformation is a linear combination of six spectral bands of Landsat ETM+ data that results in three components: wetness, greenness, and brightness. These three components have been useful in image analysis of agricultural and forested systems (Crist and Kauth 1986; Kauth and Thomas 1976).

Table 2. Vegetation indices used for correlations and regressions with field metrics. The band (B) refers to the Landsat 7 ETM+ band order (B_1 = blue, B_2 = green, B_3 = red, B_4 = NIR, B_5 = SWIR1, B_7 = SWIR2).

	Index and abbreviation	Formula	Reference
Red – NIR veg. indices	Simple Ratio (SR)	$\frac{B_4}{B_3}$	Jordan 1969
	normalized difference vegetation index (NDVI)	$\frac{B_4 - B_3}{B_4 + B_3}$	Rouse et al. 1973; Tucker 1979
	Soil Adjusted Vegetation Index (SAVI)	$\frac{B_4 - B_3}{B_4 + B_3 + 0.5}(1 + 0.5)$	Huete 1988
	Renormalized Difference Vegetation Index (RDVI)	$\frac{B_4 - B_3}{\sqrt{(B_4 + B_3)}}$	Roujean and Breon 1995; Haboudane et al. 2004
	Modified Triangular Vegetation Index 1 (MTVI1)	$1.2[1.2\,(B_4 - B_2) - 2.5(B_3 - B_2)]$	Haboudane et al. 2004
Green/SWIR1 veg. indices	Plant Senescence Reflectance Index (PSRI)	$\frac{B_3 - B_2}{B_4}$	Merzlyak et al. 1999
	Canopy Index (CI)	$B_5 - B_2$	Vescovo and Gianelle 2008
	Normalized Canopy Index (NCI)	$\frac{B_5 - B_2}{B_5 + B_2}$	Vescovo and Gianelle 2008
	Ratio Cover Index (RCI)	$\frac{B_5}{B_3}$	Zhang and Guo 2008
	Normalized Difference Cover Index (NDCI)	$\frac{B_5 - B_3}{B_5 + B_3}$	Zhang and Guo 2008
	normalized difference water index (NDWI)	$\frac{B_4 - B_5}{B_4 + B_5}$	Hardisky, Smart, and Klemas 1983; Gao 1996
SWIR 2 veg. indices	Seven/Four ratio	$\frac{B_7}{B_4}$	
	Normalized Difference Infrared Index 7 (NDII7)	$\frac{B_4 - B_7}{B_4 + B_7}$	Hardisky, Smart, and Klemas 1983
	Soil Adjusted Total Vegetation Index (SATVI)	$\frac{B_5 - B_3}{B_5 + B_3 + 0.5} \times (1 + 0.5)(B_7/2)$	Marsett et al. 2006
Tasselled cap	Brightness Index (BI)	$0.2043 \times B_1 + 0.4158 \times B_2 + 0.5524 \times B_3 + 0.5741 \times B_4 + 0.3124 \times B_5 + 0.2303 \times B_7$	Crist 1985
	Greeness Index (GVI)	$-0.1603 \times B_1 - 0.2819 \times B_2 - 0.4934 \times B_3 + 0.7940 \times B_4 - 0.0002 \times B_5 - 0.1446 \times B_7$	Crist 1985
	Wetness Index (WI)	$0.0315 \times B_1 + 0.2021 \times B_2 + 0.3102 \times B_3 + 0.1594 \times B_5 - 0.6806 \times B_5 - 0.6109 \times B_7$	Crist 1985

2.7. *Analysis*

All biophysical vegetation and remotely sensed data was tested for normality using the Lilliefors test (Lilliefors 1967). Non-normal data distributions were normalized and Pearson's correlations were computed between the utilization at each site and the vegetation metrics of vertical structure, biomass, and foliar cover for each sampling bout. Pearson's correlations were also performed between all the remotely sensed data and vertical structure, cover, and biomass for each sampling bout. Correlation coefficients (r) with $p \leq 0.05$ were considered significant.

To increase the potential predictive power of satellite data to explain the variance in vegetation metrics, multiple regression techniques were employed. Following Hudak et al. (2006), full, stepwise, and best-subset models were created to determine the best predictor variables to model structure, cover, and biomass for each sampling bout. Using both the stepwise and best-subset modelling techniques helped to ensure that multiple models were explored for the best fit by searching different pathways for variable selection (Hudak et al. 2006). We used a stepwise technique that selects the model with the lowest Akaike information criterion (AIC) (Akaike 1974) by searching both forward and backward pathways (Hudak et al. 2006). Next, a best-subset method was performed to search all possible pathways, choosing the best variables for a defined number of predictor variables (Hudak et al. 2006). Models with the lowest corrected AIC (Sugiura 1978) having a variance inflation factor (VIF) less than 10 (Friendly and Kwan 2009) were selected as the 'best' models. We further tested all residuals for a normal distribution with a mean of zero and for spatial autocorrelation using Moran's *I* (Cliff and Ord 1981). Models selected from each bout for each vegetation metric were then applied to all other bouts to explore the ability for these best models to predict vegetation amounts at different phenological stages.

Using the selected best regression models, we then computed and mapped the estimated foliar cover, biomass, and vegetation structure metric for each Landsat grid cell across all the pasture's suitable habitat analysis area for each sample bout scene. This produced three maps for each vegetation metric – one representing each of the three sampling bouts. To compare the mean estimated vegetation amounts of cover, biomass, and structure by stocking rate (control, low, medium, and high) across the sampling bouts, we generated a 95% confidence interval around the mean using a bootstrapping resampling procedure. This bootstrap procedure computes a mean from randomly selected samples with replacement from the data set in question until it equals the number of samples of the original data set, then this is repeated 1000 times producing 1000 means. The 95% confidence interval of the mean is constructed by selecting the 2.5 and 97.5 percentiles. Where the confidence intervals around the mean for each stocking rate do not overlap, significant differences exist at the 95% confidence level. To quantify the effects of stocking rate on each of the predicted vegetation metrics, ordinary least square (OLS) regression was performed using the pasture stocking rate (AUM ha $^{-1}$) as the predictor variable and mean vegetation amount by pasture as a response variable. The slope of each OLS regression indicates the effect of stocking rate on each vegetation amount.

3. Results

3.1. *Data exploration of biophysical variables*

Forage utilization ranged from 0 to 35%. Utilization rates in high and medium treatment pastures were significantly higher than control pastures ($p < 0.001$). There were no significant differences in utilization between high and medium stocking rates ($p = 0.38$). Forage utilization was negatively correlated to all three vegetation metrics across all sampling bouts (Figure 4). Utilization was most strongly correlated with cover during the second sampling bout (correlation coefficient $r = -0.69$). Relationships between structure and utilization varied the least across the three sampling periods, with r values ranging from −0.62 to −0.66. Biomass had

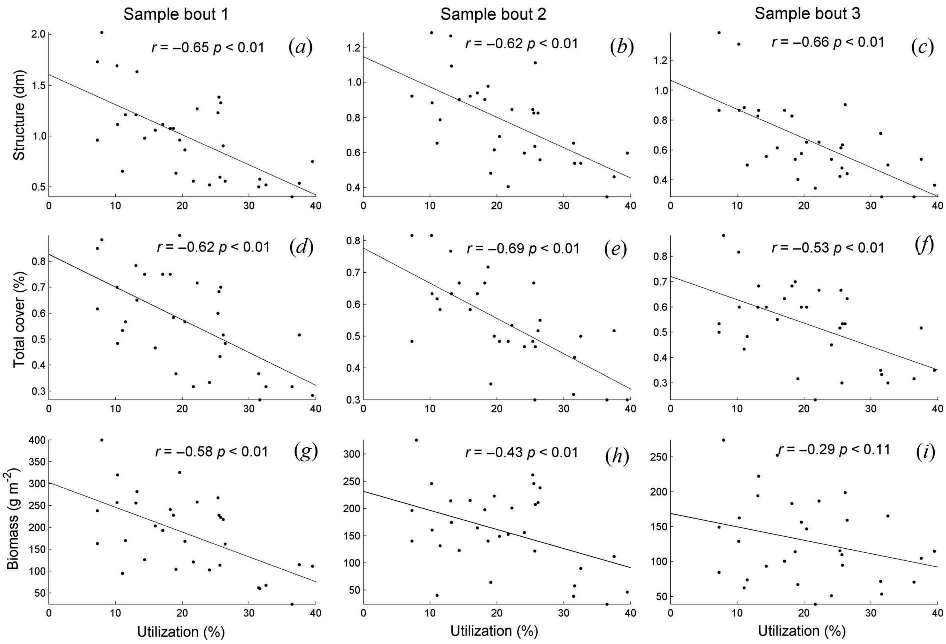

Figure 4. Pearson's correlations between end-of-year % utilization and biophysical monitoring metrics: (*a–c*) vertical structure (dm), (*d–f*) cover (%), and (*g–i*) dry biomass (g m^{-2}).

the weakest correlations to utilization, with decreasing relationships observed later in the growing season (Figure 4).

3.2. *Relationships between satellite data and biophysical vegetation measures*

The relationships between the biophysical data and satellite indices had Pearson's correlation coefficient (r) values ranging from −0.75 to +0.74 (Table 3). Band 7, the seven/four ratio, and NDII7 were consistently significantly correlated across the growing season to structure, canopy cover, and biomass. The strongest relationships were between cover and the seven/four ratio and NDII7 vegetation indices, all having absolute r values >0.63 (Table 3). The relationships between satellite data and biomass and structure were also significant but were more weakly correlated than for cover. For structure, Band 7 and the seven/four ratio had the highest correlations, with r values ranging from −0.44 to −0.58 across the sampling bouts. Biomass was most correlated to the seven/four ratio or NDII7, having similar results to vertical structure (r values ranging from −0.52 to −0.66) in each sample bout across the growing season.

3.3. *Multiple regression modelling*

Fitting the full, stepwise, and best-subset models to the biophysical vegetation metrics for each sample bout revealed multicollinearity with the predictor variables. The full model and stepwise models for all three vegetation metrics had higher coefficient of determination (R^2) values and lower corrected AIC values than the best-subset models,

Table 3. Pearson's correlation coefficient values (*r*) between the remotely sensed data and the vegetation field metrics structure, cover, and dry biomass across the three sampling periods. Values in bold are significant at the 0.05 *p*-value; only spectral predictors with at least one significant relation to any field metric are included in the table.

	Pearson's correlation coefficient value (*r*)								
	Structure			Cover			Biomass		
Remotely sensed band or index	1 July	12 August	1 October	1 July	12 August	1 October	1 July	12 August	1 October
Band 4	0.33	0.15	0.17	**0.44**	0.33	**0.58**	**0.40**	**0.46**	**0.43**
Band 7	**−0.44**	**−0.53**	**−0.58**	**−0.60**	**−0.66**	**−0.48**	**−0.43**	**−0.48**	**−0.41**
SR	−0.23	0.23	0.27	**−0.47**	**0.43**	**0.46**	−0.27	**0.51**	**0.45**
NDVI	0.22	−0.31	0.26	**0.46**	**−0.48**	**0.46**	0.26	**−0.54**	**0.44**
SAVI	0.27	0.16	0.27	**0.47**	**0.38**	**0.57**	0.33	**0.48**	**0.51**
RDVI	0.26	0.16	0.27	**0.47**	**0.38**	**0.57**	0.31	**0.48**	**0.51**
MTVI1	0.24	0.14	0.21	**0.43**	**0.36**	**0.51**	0.30	**0.47**	**0.46**
NCI	**−0.42**	0.20	0.08	**−0.35**	0.29	0.18	−0.34	**0.41**	0.20
PSRI	−0.13	0.18	0.28	**−0.37**	−0.05	0.23	−0.14	−0.22	0.23
SATVI	0.04	0.31	0.18	0.27	**0.42**	0.33	0.13	**0.58**	0.23
Seven/Four ratio	**−0.49**	**−0.48**	**−0.54**	**−0.66**	**−0.68**	**−0.75**	**−0.52**	**−0.66**	**−0.57**
NDII7	**0.46**	**0.46**	**0.54**	**0.63**	**0.66**	**0.74**	**0.49**	**0.65**	**0.58**
NDWI	**0.35**	0.18	**0.39**	**0.53**	**0.45**	**0.55**	**0.39**	**0.44**	**0.50**
TC − GVI	0.30	0.24	**0.37**	**0.49**	**0.46**	**0.67**	**0.37**	**0.52**	**0.57**
TC − WI	**0.39**	0.32	**0.47**	**0.54**	**0.43**	0.24	**0.38**	0.19	0.26

but the predictor variables were highly collinear. The best-subset models exhibited decreased adjusted-R^2 values when compared to the full and stepwise, but met the assumption that the predictor variables were independent and therefore more appropriate models (Table 4). Each selected best-subset OLS model had normally distributed residuals with a mean of zero and exhibited no significant spatial autocorrelation when tested with Moran's *I* (Cliff and Ord 1981).

The best-subset models for all three vegetation metrics had statistically significant ($p \leq 0.01$) relationships between satellite data and biophysical data estimates. While all models were statistically significant, the coefficient of determination (R^2) was wide-ranging and below 0.75 for all subset models selected. The best-subset regression models for structure and biomass had an explained variance that decreased with each successive sampling bout as the growing season progressed and the grassland senesced. The selected models' adjusted-R^2 values for vertical structure estimation decreased from 0.70 in the first sampling bout to 0.35 in the third, while the biomass estimation across the sampling bouts decreased from 0.65 in in the first sampling bout to 0.32 in the third. The selected best-subset models for cover performed better across the growing season, having an adjusted-R^2 greater than 0.60 for each sampling bout (Figure 5). Using the best model for each sampling bout to predict the vegetation amount collected during any other sampling bout indicated that no single model could achieve the best relationship across the growing season (Figure 5). For example, the adjusted-R^2 value decreased when using the best-subset model selected for cover during the first sampling bout to model cover for the third sampling bout, from 0.67 to 0.50.

3.4. *Sensitivity to stocking rate*

The best-subset model outputs showed that while within-pasture heterogeneity in predicted vegetation amounts existed across the study area (Figure 6), statistical differences by

Table 4. Selected regression models for each vegetation metric and bout. Full, stepwise and the selected best subset models are shown. The 'best' subset models, shown in bold, were selected based on the lowest corrected AIC (AICc) and an acceptable variance inflation factor (VIF < 10) from all candidate models created (not shown). The significance levels for each predictor variable are shown within the table: $p < 0.001$, $p < 0.01$, $p < 0.05$, $p < 0.1$, and NS denotes not significant. Only spectral predictors that were selected as significant in any one of the models were included in the table.

Field metric	Model	Sample bout	Intercept	B1	B2	B3	B4	B5	B7	SR	NDVI	SAVI	RDVI	MTVII	NCI	RCI	NDCI	PSRI	SATVI	Seven/Four ratio	NDII7	NDWI	R^2	Adj. R^2	Residual SE	AICc	p-value	Parameter with a VIF value over 10
Structure	Full	1	NS	NS	NS	NS	NS	NS	NS	NS	NS	NS	NS	NS	NS	NS	NS	NS	NS	NS	NS	NS	0.84	0.63	0.25	185.41	0.01	Yes
	Stepwise	1	0.1	NS				0.1		0.1	0.05		0.05				0.05		0.05	0.05			0.82	0.7	0.23	31.72	9.70E-05	Yes
	Best subset	1	**0.001**	**0.001**									**0.001**							**0.001**			**0.73**	**0.7**	**0.23**	**2.77**	**4.10E-06**	**No**
	Full	2	NS	NS	NS	NS	NS	NS	NS	NS	NS	NS	NS	NS	NS	NS	NS	NS	NS	NS	NS	NS	0.76	0.35	0.2	237.01	1.40E-01	Yes
	Stepwise	2	0.05			NS	NS	0.1	0.1		NS	NS	NS			0.1	0.1		0.1		0.1	0.1	0.75	0.57	0.16	14.24	4.00E-03	Yes
	Best subset	2	**0.001**																	**0.001**		**0.001**	**0.52**	**0.48**	**0.18**	**−13.66**	**5.40E-05**	**No**
	Full	3	NS	NS	NS	NS	NS	NS	NS	NS	NS	NS	NS	NS	NS	NS	NS	NS	NS	NS	NS	NS	0.66	0.19	0.27	188.52	2.70E-01	Yes
	Stepwise	3	0.05							0.1	0.1	0.1	NS		0.05	NS		0.05		NS	NS	0.05	0.63	0.46	0.22	16.87	6.50E-03	Yes
	Best subset	3	**0.001**					**NS**	**0.001**														**0.39**	**0.35**	**0.24**	**4.67**	**7.80E-04**	**No**
Cover	Full	1	NS	NS	NS	NS	NS	NS	NS	NS	NS	NS	NS	NS	NS	NS	NS	NS	NS	NS	NS	NS	0.82	0.57	0.12	138.27	1.50E-02	Yes
	Stepwise	1	0.05		0.1	0.1	0.1	0.1			0.1	0.1	0.1			0.1		0.1		NS	0.1	0.05	0.81	0.69	0.1	−22.94	1.40E-04	Yes
	Best subset	1	**0.001**					**0.05**						**0.001**						**0.001**			**0.7**	**0.67**	**0.11**	**−45.57**	**1.50E-07**	**No**
	Full	2	NS	NS	NS	NS	NS	NS	NS	NS	NS	NS	NS	NS	NS	NS	NS	NS	NS	NS	NS	NS	0.83	0.6	0.1	155.2	1.20E-02	Yes
	Stepwise	2	NS	0.05		0.01	0.01		NS	0.01			0.01						0.05		0.1	0.01	0.81	0.72	0.08	−31.13	1.40E-05	Yes
	Best subset	2	**0.001**									**0.001**								**0.001**			**0.64**	**0.62**	**0.1**	**−52.11**	**3.30E-07**	**No**
	Full	3	NS	0.1	NS	NS	NS	NS	NS	NS	NS	NS	NS	NS	NS	NS	NS	NS	NS	NS	NS	NS	0.81	0.55	0.11	129.83	2.10E-02	Yes
	Stepwise	3	NS	0.05	NS	NS		0.1	0.05		NS	NS	NS			NS		NS	0.05			0.05	0.8	0.64	0.09	−18.14	1.30E-03	Yes
	Best subset	3	**0.001**													**0.001**			**0.001**				**0.67**	**0.64**	**0.09**	**−54.57**	**1.20E-07**	**No**
Biomass	Full	1	NS	NS	NS	0.05	0.05	NS	NS	0.1	0.01	0.01	0.05	NA	0.001	0.05	NS	0.01	NS	NS	0.5	0.01	0.9	0.75	44.46	516.27	1.90E-03	Yes
	Stepwise	1	NS			0.01	0.01	0.01	0.01	0.05	0.01	0.01	0.01		0.001	0.01		0.001		0.01	0.01	0.01	0.88	0.79	41.09	365.08	2.40E-05	Yes
	Best subset	1	**0.001**															**0.001**		**0.001**			**0.67**	**0.65**	**52.49**	**349.99**	**8.70E-08**	**No**
	Full	2	NS	NS	NS	0.1	0.1	NS	NS	0.05	0.1	0.1	0.1	NA	NS	NS	0.1	NS	NS	NS	0.05	0.05	0.85	0.65	43.75	515.24	5.70E-03	Yes
	Stepwise	2	0.05	NS	NS	0.01	0.01	0.05	0.05	0.05	0.01	0.01	0.01			0.05	0.05	NS		NS	0.01	0.05	0.85	0.69	41.2	384.27	1.20E-03	Yes
	Best subset	2	**0.001**																	**0.001**		**0.01**	**0.57**	**0.54**	**50.26**	**347.22**	**5.00E-06**	**No**
	Full	3	NS	NS	NS	NS	NS	0.05	0.05	NS	NS	NS	NS	NA	NS	NS	NS	NS	0.05	0.01	NS	NS	0.83	0.57	39.86	527.04	2.30E-02	Yes
	Stepwise	3	0.1		NS	0.001	0.001	0.001	0.001	0.001	0.001		0.001				0.001	NS	0.001	0.001		0.1	0.81	0.67	34.83	351.48	6.10E-04	Yes
	Best subset	3	**0.001**																		**0.001**		**0.35**	**0.32**	**49.86**	**334.71**	**5.00E-04**	**No**

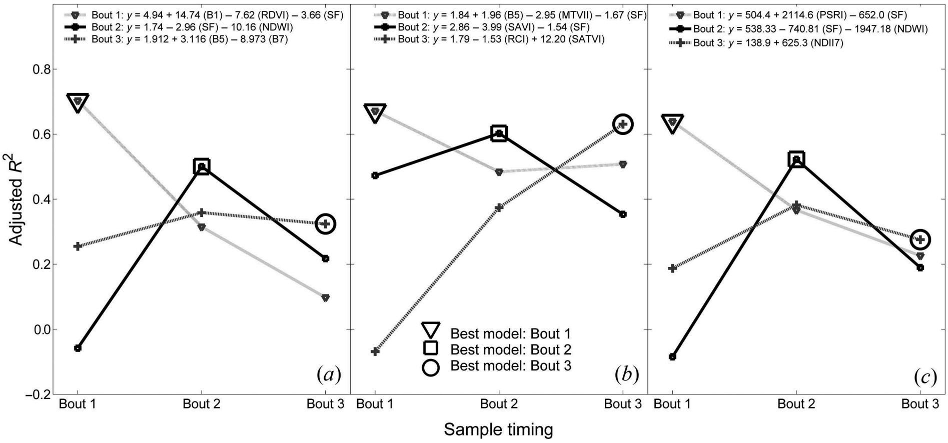

Figure 5. Adjusted R^2 values from the selected best subset regression models for each sampling bout and vegetation metric: (*a*) vertical structure, (*b*) foliar cover, and (*c*) biomass. The best model from each sampling bout is then used to predict the vegetation metric at the two other sampling bouts.

stocking rate were evident (Figure 7). Limiting the comparison to the suitable habitat analysis area, control pastures had significantly higher predicted structure, cover, and biomass than all grazed areas; pastures with high stocking rates had the lowest predicted vegetation amounts across all sampling bouts (Figure 7). The treatment areas stocked at low and medium rates largely had mean predicted vegetation quantities falling between the high and control treatment means across the growing season. In the first sampling bout, the medium stocking rate treatment area had higher predicted vegetation amounts for structure and biomass than the low treatment area, but lower predicted vegetation amounts for the second and third sampling bouts (Figure 7). This is likely attributed to the timing of grazing in one of the medium pastures happening during and after the first sampling bout.

Estimates of vegetation quantity by pasture stocking rate indicated significant trends in the reduction of vegetation across the gradient of stocking rates (Figure 8). This reduction in vegetation is subsequently observed across all bouts. Depending on time of year, for each extra AUM ha^{-1}, biomass was reduced in the range 63 g m^{-2} (sampling bout 1) to 38 g m^{-2} (sampling bout 3) (Figure 8). Vertical structure was also reduced by between 0.17 and 0.31 decimetres with an increase of 1 AUM ha^{-1} in grazing stocking rate depending on the time of measurement, with the greatest reduction observed in the first sampling bout (Figure 8). Compared to structure and biomass, the reduction of cover across the grazing gradient was more consistent across the growing season, with a measure of between 11 and 13% with each additional AUM ha^{-1} (Figure 8).

4. Discussion

Analysis of vegetation amounts across the sampling periods of 2012 showed reduced vegetation in areas with greater stocking rates. These findings provide evidence that our remote sensing-based models were sensitive enough to discern different stocking rates across the summer and fall months when cattle are grazing. However, the models most strongly correlated to vegetation metrics changed over the course of the study period as

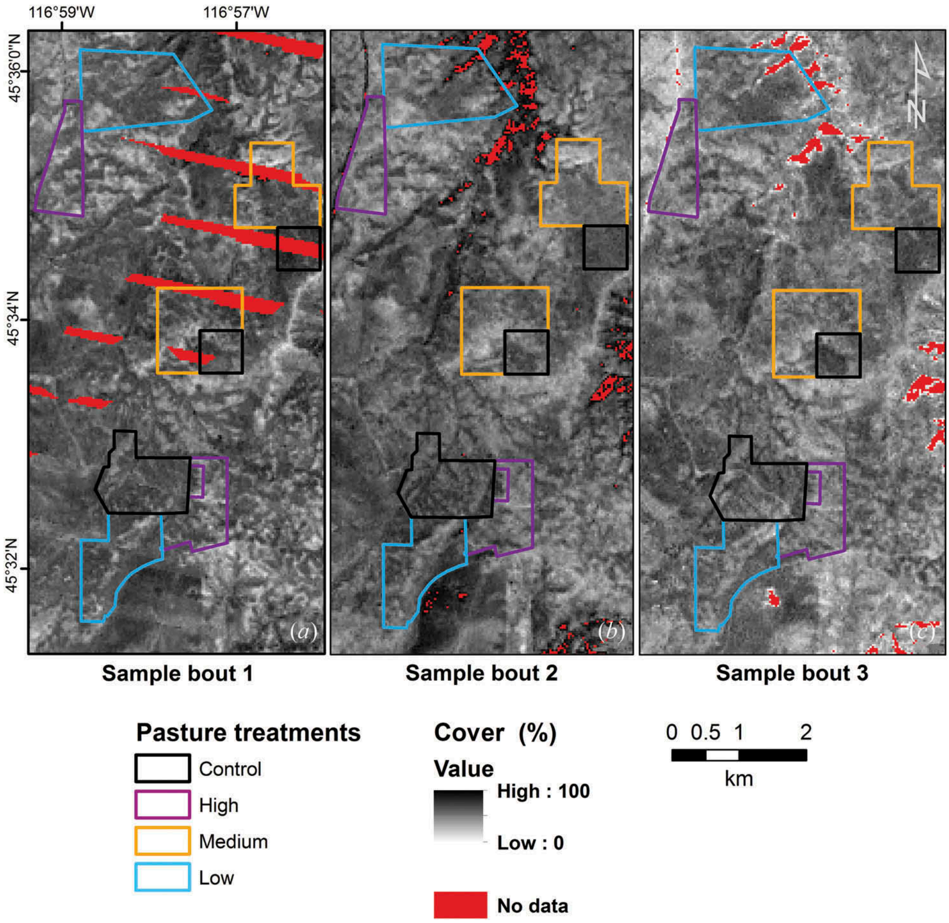

Figure 6. Maps of vegetation cover (%) by sampling bout across the grazing treatment pasture. No data, or values outside of the regression equation range of estimation, are shown in red.

the grassland vegetation senesced, suggesting that there was no temporally consistent single best model to monitor grazing effects using the remotely sensed indices tested in this grassland system. Creating models that use vegetation indices and bands that most appropriately match up with phenology (i.e. live or senescent vegetation) improved model explanatory power to predict common rangeland monitoring metrics.

Relating our field measures of vertical structure, cover, and biomass with grazing intensity as measured by end-of-year utilization validated that vegetation amounts changed with higher stocking rates. Finding significant correlations between our vegetation metrics and the utilization metric helps clarify that our models can be used to quantify changes in vegetation due to grazing, and not just loss due to changes in phenology and non-herbivory related defoliation. From these data we observed significant negative correlations between vegetation metrics across the grazing season and utilization. Our result showing that vertical structure is sensitive to utilization corroborates the finding of Johnson et al. (2011) that vegetation structure was significantly reduced with increased stocking rates in treatment years, as well as one year after grazing. Cover and biomass were also negatively correlated in

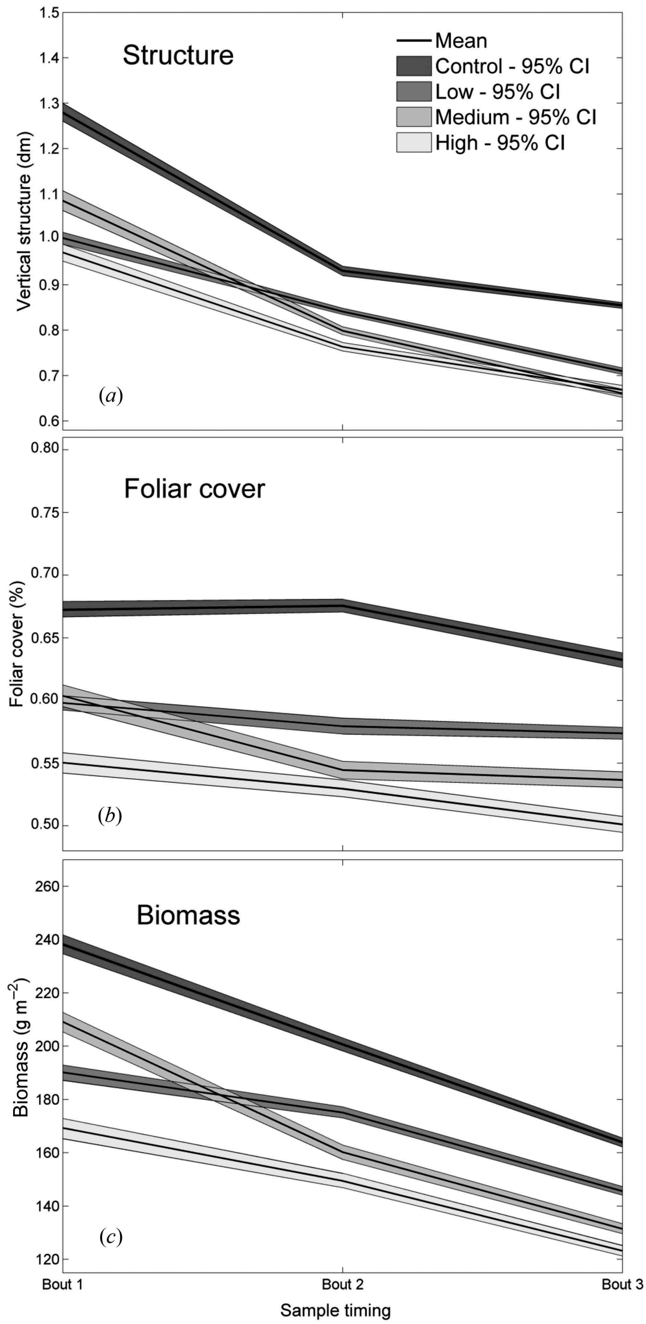

Figure 7. Predicted vegetation amounts for (*a*) structure, (*b*) foliar cover, and (*c*) biomass across the growing season by stocking rate. Mean vegetation amounts are shown as solid lines, with the filled shaded area showing the 95% confidence interval around the mean. Predicted vegetation amounts were derived from multiple regression analysis by stocking rate and sample bout.

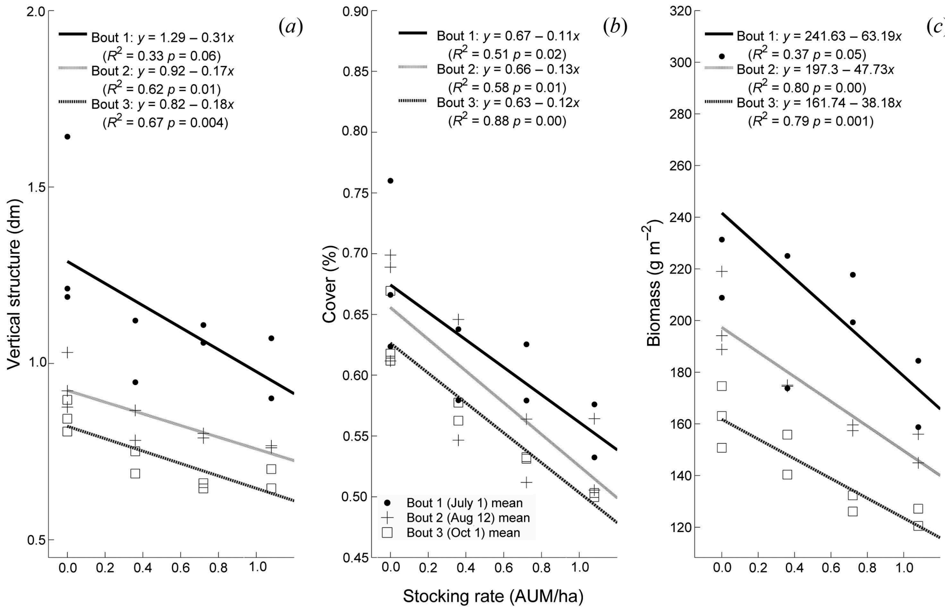

Figure 8. Effect of stocking rate on (*a*) vertical structure, (*b*) foliar cover, and (*c*) biomass by sampling bout. The point symbols represent the mean pasture biophysical estimate by sampling bout. The ordinary least square (OLS) regression lines show the effect of the stocking rate (animal unit month [AUM] ha^{-1}) on the pasture means for each sampling bout. The solid black line and black symbol refer to sampling bout one (SB1) data; the grey line and plus symbol refer to sample bout two (SB2) data; the dotted line and box refer to sampling bout three data (SB3) data.

all but one comparison across the three sample bouts, providing evidence that grazing can affect vegetation amounts across the growing season.

Both the Pearson's correlations and multiple regression models between vegetation data and remotely sensed data indicated that vegetation indices with bands 4 and 7 were the most useful to explain our biophysical vegetation measurements. When performing Pearson's correlation, the seven/four ratio and NDII7 best predicted vegetation monitoring metrics across the three different sampling periods. Vegetation indices that included band 7 were most often selected using the subset regression approach when finding the 'best' models. One explanation is that band 7 is sensitive to soil and vegetation moisture; greater reflectance occurs when plants and soils are dry and more bare ground is present (Knipling 1970; Tucker 1980). As SAVI also is sensitive to bare ground, the stronger relationships of field metrics to indices incorporating SWIR suggest that live plant moisture levels and the amount of non-photosynthetic vegetation were more important than bare ground. Band 7 may be indicative of grazing levels and resulting impacts on the amount of bare ground and vegetation moisture, with higher grazing intensities creating drier, more barren areas. The lack of strong correlations with greenness indices is similar to other studies that have tracked NDVI at different points in a growing season (e.g. Butterfield and Malmström 2009; Schino et al. 2003; Vescovo and Gianelle 2008). Within the bunchgrass ecosystem, NDVI had high r values ($r > 0.7$) for green vegetation and green cover, but lacked strong correlations with the selected biophysical variables throughout the year as vegetation senesced. The result that vegetation indices containing bands 5 and 7 outperformed NDVI or SAVI across the growing season, especially when grasses had senesced, is similar to the findings of Numata et al. (2007) when assessing vegetation parameters during the dry season in Brazil.

As the 2012 growing season progressed, the models created using the best-subset approach decreased in explanatory power, but remained statistically significant. Cover was the biophysical metric exhibiting the greatest explained variance across the growing season using both Pearson's correlations and the best-subset regression models. This indicates that a estimated of cover could be the most useful metric for setting management objectives or performing multiyear trend analysis. Cover has been found to be a reliable measure when estimated by satellite and is a commonly used metric to assess rangeland condition in many grassland habitats (Booth and Tueller 2003; Hagen et al. 2012) and on the Zumwalt Prairie. Biomass and vertical structure vegetation metrics are more difficult to estimate as the growing season progresses. Increasing the ability to model vegetation later in the growing season could also be explored with other analytic techniques. Numata et al. (2007) found that using fraction images of non-photosynthetic vegetation produced from multiple endmember spectral mixture analysis (MESMA) (Roberts, Smith, and Adams 1993) had the highest correlation to grazing intensity.

For analytic simplicity and creation of management tools, a single vegetation index would provide all the needed information to monitor the selected biophysical metric across the year (Marsett et al. 2006); however, the best-subset model selection showed that accuracy is improved by producing models that match vegetation phenology. As others have found, the ability to explain field vegetation metrics with remote-sensing data decreases as vegetation senesces (Butterfield and Malmström 2009; Schino et al. 2003). This has been attributed to the reduction of amount of green vegetation *versus* senesced vegetation impacting the spectral signal and subsequent green vegetation indices (Butterfield and Malmström 2009; Hardisky, Smart, and Klemas 1983; Numata et al. 2007; Schino et al. 2003; Todd, Hoffer, and Milchunas 1998; Vescovo and Gianelle 2008). In this study we found that macro-plot level field data for cover, biomass, and structure became more similar over the course of the growing season, reducing the variation of vegetation data being modelled. With increasing similarity and the amount of variance to be explained decreasing, coupled with a small sample size (N = 32) for each sampling bout, the statistical relationships between field and remote-sensing data become less robust later in the year specifically for vegetation biomass and structure.

While our study highlights the potential to monitor grazing effects by satellite across the grazing season in this bunchgrass ecosystem, it has limitations. First, our highest utilization rate at any given macro-plot was just over 35%, a rate that is not considered very high for the Zumwalt Prairie habitat (Holechek et al. 1999; Skovlin et al. 1976). Therefore, the models created in this study to estimate vertical structure, biomass, and cover are best suited for moderate levels of grazing and would likely be improved with more variance in grazing levels. Future studies would benefit from sampling sites with higher variation in forage utilization across the landscape. Second, field parameter estimation of biomass proved difficult in such a highly heterogeneous landscape with limited samples (Friedl et al. 1994). Estimation could be improved with more sub-samples within the 30 × 30 macro-plot or a different technique of field estimation of biomass. Other studies have sampled larger areas in the field; for example, Marsett et al. (2006) had field sites of 90 m × 150 m helping to ensure the field-sampled data were co-registered to only pixels within the field sample area. Third, factors such as the scan line errors across all dates and cloud cover in the early part of the study period created the need to acquire Landsat scenes from multiple dates to correlate with field measures, potentially introducing noise into the analysis due to phenological differences between selected remote-sensing scenes. However, a supplemental analysis of correlations between scene dates within bouts and greenness over the season showed minimal differences (all r values >0.89) in phenology within bouts, and considerable differences in site phenology between bouts (Figure 3), suggesting that our gap-fill methodology did not overly impact our results.

Finally, inter-annual variation in phenology and production as a result of climate and seasonality of precipitation means that these models may lose their effectiveness in years where meteorological conditions are considerably different. This highlights the need to collect field data over multiple years to improve model robustness for long-term monitoring. For example, in 2012 the total annual precipitation was 96% of normal for the year, but only 67 % of normal for the summer months (June–August). Additional field data collection is the goal of a future study.

Future research should focus on automation of this analysis framework in understanding how climate influences vegetation production phenology, such as timing of peak greenness or senescence across the site. Because the ability of vegetation indices to accurately estimate vegetation amounts is dependent on vegetation phenology (Butterfield and Malmström 2009; Vescovo and Gianelle 2008), application of the models in future years may be performed by selecting the model that most appropriately aligns with the current phenology (Figure 9). This could be done using an NDVI curve derived from MODIS, with

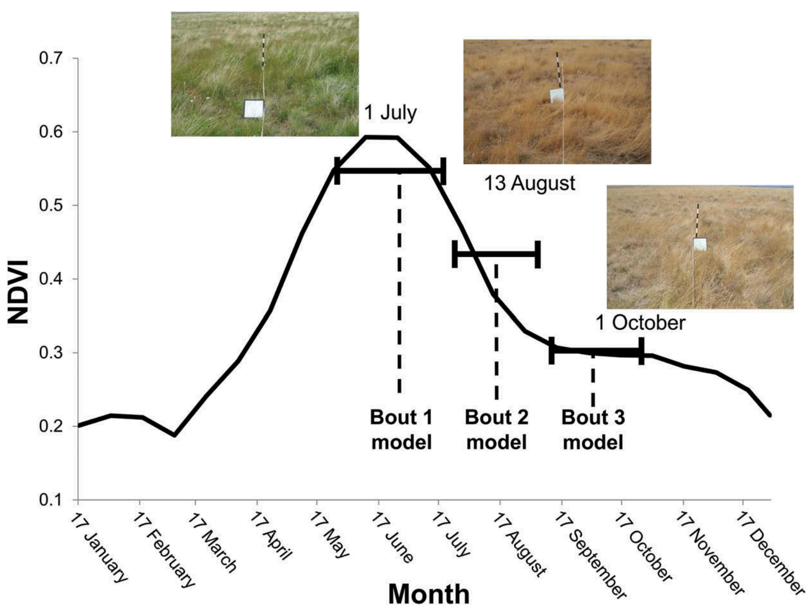

Figure 9. The mean 2000–2012 MODIS normalized difference vegetation index (NDVI) curve derived from the 16-day MODIS NDVI product, with the theoritical timeframe for most appropriate model selection for future years represented by black bars. The pictures with associated dates show what the vegetation looked like at each given time period.

model selection being based on that part of the curve for which the models are best suited. For example, the model developed for the first sampling bout is best suited around peak greenness, while the model developed for the third sampling bout aligns with fully senescent vegetation. Providing near-real-time maps of important biophysical measures for management decision making will depend on automation of this process. This could be achieved by utilizing Landsat Ecosystem Disturbance Adaptive Processing System (LEDAPS) at-surface reflectance products (Masek et al. 2006) with the associated automated data analysis code that creates user-friendly maps or interactive analysis products for rangeland managers. Future studies may also benefit by scaling the analysis up to MODIS resolution, to determine whether this sensor also has the ability to monitor grazing intensity, which would potentially increase the feasibility to create more frequent within-season measures of important grassland monitoring metrics.

5. Conclusions

Rangeland managers need timely and accurate landscape-scale estimates of vegetation amounts to determine the effects of their land management decisions. Prior remote-sensing studies of grazing metrics have largely sought to estimate vegetation amounts during peak greenness. Here we show that remotely sensed measures of vegetation are sensitive to the varying amounts of grazing across the study period. We also demonstrate that models built only on sampling during peak greenness are not applicable across the entire grazing season as vegetation senesces, and that models should change across the season to capture senescence. This research provides a better understanding of the feasibility of producing multiple, within-season, near-real-time remotely sensed data-driven grazing management decision-support tools.

Acknowledgements

We thank all the individuals who assisted with the collection of field data and The Nature Conservancy NE Oregon field office staff. We are grateful to J.D. Wulfhorst, Arjan Meddens, and Scott Butterfield for insightful editorial comments during the writing of this manuscript. We also would like to thank the two anonymous reviewers and the Editor for valuable feedback, which greatly improved the manuscript.

Disclosure statement

No potential conflict of interest was reported by the authors.

Funding

This research was completed with support from National Aeronautics and Space Administration (NASA) [grant number NNX10AT77A]; NSF Idaho EPSCoR [grant number EPS-0814387]; NSF GK-12 [grant number DGE – 0841199]; and The Nature Conservancy (TNC) Zumwalt Prairie preserve.

References

Akaike, H. 1974. "A New Look at the Statistical Model Identification." *IEEE Transactions on Automatic Control* 19 (6): 716–723. doi:10.1109/TAC.1974.1100705.

Anderson, E. W., and W. F. Currier. 1973. "Evaluating Zones of Utilization." *Journal of Range Management* 26 (2): 87–91. doi:10.2307/3896457.

Archer, E. R. M. 2004. "Beyond the 'Climate Versus Grazing' Impasse: Using Remote Sensing to Investigate the Effects of Grazing System Choice on Vegetation Cover in the Eastern Karoo." *Journal of Arid Environments* 57: 381–408. doi:10.1016/S0140-1963(03)00107-1.

Bartuszevige, A. M., P. L. Kennedy, and R. V. Taylor. 2012. "Sixty-Seven Years of Landscape Change in the Last, Large Remnant of the Pacific Northwest Bunchgrass Prairie." *Natural Areas Journal* 32: 166–170. doi:10.3375/043.032.0205.

Blanco, L. J., C. A. Ferrando, and F. N. Biurrun. 2009. "Remote Sensing of Spatial and Temporal Vegetation Patterns in Two Grazing Systems." *Rangeland Ecology & Management* 62 (5): 445–451. doi:10.2111/08-213.1.

Booth, D. T., and P. T. Tueller. 2003. "Rangeland Monitoring Using Remote Sensing." *Arid Land Research and Management* 17: 455–467. doi:10.1080/713936105.

Bradley, B. A., and M. T. O'sullivan. 2011. "Assessing the Short-Term Impacts of Changing Grazing Regime at the Landscape Scale with Remote Sensing." *International Journal of Remote Sensing* 32 (20): 5797–5813. doi:10.1080/01431161.2010.507680.

Brinkmann, K., U. Dickhoefer, E. Schlecht, and A. Buerkert. 2011. "Quantification of Aboveground Rangeland Productivity and Anthropogenic Degradation on the Arabian Peninsula Using Landsat Imagery and Field Inventory Data." *Remote Sensing of Environment* 115 (2): 465–474. doi:10.1016/j.rse.2010.09.016.

Butterfield, H. S., and C. M. Malmstrom. 2006. "Experimental Use of Remote Sensing by Private Range Managers and Its Influence on Management Decisions." *Rangeland Ecology & Management* 59 (5): 541–548. doi:10.2111/05-184R1.1.

Butterfield, H. S., and C. M. Malmström. 2009. "The Effects of Phenology on Indirect Measures of Aboveground Biomass in Annual Grasses." *International Journal of Remote Sensing* 30 (12): 3133–3146. doi:10.1080/01431160802558774.

Chander, G., B. L. Markham, and D. L. Helder. 2009. "Summary of Current Radiometric Calibration Coefficients for Landsat MSS, TM, ETM+, and EO-1 ALI Sensors." *Remote Sensing of Environment* 113 (5): 893–903. doi:10.1016/j.rse.2009.01.007.

Chapin, F. S., S. Diaz, M. Howden, J. Puigdefabregas, M. S. Smith, T. Benning, F. Bryant, B. Campbell, J. DuToit, K. Galvin, E. Holland, L. Joyce, A. K. Knapp, P. Matson, R. Miller, D. Ojima, W. Polley, T. Seastedt, A. Suarez, T. Svejcar, and C. Wessman. 1996. "Rangelands in a Changing Climate: Impacts, Adaptations and Mitigation." In *Climate Change 1995 Impacts, Adaptations and Mitigation of Climate Change: Scientific-Technical Analyses*, eds. R. T. Watson, M. C. Zinyowera, and R. G. Moss, 135–158. Cambridge: Intergovernmental Panel on Climate Change, Cambridge Univ. Press.

Chavez, P. 1996. "Image-Based Atmospheric Corrections - Revisited and Improved." *Photogrammetric Engineering and Remote Sensing* 62 (9): 1025–1036.

Cliff, A. D., and J. K. Ord. 1981. *Spatial Processes,Models and Applications*. London, UK: Pion.

Conner, R., A. Seidl, L. VanTassell, and N. Wilkins. 2002. *United States Grasslands and Related Resources: An Economic and Biological Trends Assessment*. College Station: Texas A&M Institute of Renewable Natural Resources.

Coulloudon, B., K. Eshelman, J. Gianola, N. Habich, L. Hughes, C. Johnson, M. Pellant et al. 1999. *Sampling Vegetation Attributes*. *Interagency Technical Reference*, 1731–1734. Denver, CO: U.S. Department of Interior, Bureau of Land Management.

Crist, E. P. 1985. "A TM Tasseled Cap Equivalent Transformation for Reflectance Factor Data." *Remote Sensing of Environment* 17 (3): 301–306. doi:10.1016/0034-4257(85)90102-6.

Crist, E. P., and R. J. Kauth. 1986. "The Tasseled Cap De-Mystified." *Photogrammetric Engineering and Remote Sensing* 52 (1): 81–86.

Dungan, J. 1998. "Spatial Prediction of Vegetation Quantities Using Ground and Image data." *International Journal of Remote Sensing* 19 (2): 267–285. doi:10.1080/014311698216242.

Evans, J., and R. Geerken. 2004. "Discrimination between Climate and Human-Induced Dryland Degradation." *Journal of Arid Environments* 57 (4): 535–554. doi:10.1016/S0140-1963(03)00121-6.

Friedl, M., J. Michaelsen, F. W. Davis, H. Walker, and D. S. Schimel. 1994. "Estimating Grassland Biomass and Leaf Area Index Using Ground and Satellite Data." *International Journal of Remote Sensing* 15 (7): 1401–1420. doi:10.1080/01431169408954174.

Friendly, M., and E. Kwan. 2009. "Where's Waldo? Visualizing Collinearity Diagnostics." *The American Statistician* 63 (1): 56–65. doi:10.1198/tast.2009.0012.

Gao, B. 1996. "NDWI - A Normalized Difference Water Index for Remote Sensing of Vegetation Liquid Water From Space." *Remote Sensing of Environment* 58 (3): 257–266. doi:10.1016/S0034-4257(96)00067-3.

Haboudane, D., J. R. Miller, E. Pattey, P. J. Zarco-Tejada, and I. B. Strachan. 2004. "Hyperspectral Vegetation Indices and Novel Algorithms for Predicting Green LAI of Crop Canopies: Modeling and Validation in the Context of Precision Agriculture." *Remote Sensing of Environment* 90 (3): 337–352. doi:10.1016/j.rse.2003.12.013.

Hagen, S. C., P. Heilman, R. Marsett, N. Torbick, W. Salas, J. Van Ravensway, and J. Qi. 2012. "Mapping Total Vegetation Cover across Western Rangelands with Moderate-Resolution Imaging Spectroradiometer Data." *Rangeland Ecology & Management* 65 (5): 456–467. doi:10.2111/REM-D-11-00188.1.

Hardisky, M. A., R. M. Smart, and V. Klemas. 1983. "Seasonal Spectral Characteristics and Aboveground Biomass of the Tidal Marsh Plant, Spartina alterniflora." *Photogrammetric Engineering and Remote Sensing* 49 (1): 85–92.

Henwood, W. D. 2010. "Toward a Strategy for the Conservation and Protection of the World's Temperate Grasslands." *Great Plains Research* 20: 121–134.

Herrick, J. E., V. C. Lessard, K. E. Spaeth, P. L. Shaver, R. S. Dayton, D. A. Pyke, L. Jolley, and J. J. Goebel. 2010. "National Ecosystem Assessments Supported by Scientific and Local Knowledge." *Frontiers in Ecology and the Environment* 8 (8): 403–408. doi:10.1890/100017.

Herrick, J. E., J. W. Van Zee, K. M. Havstad, L. M. Burkett, and W. G. Whitford. 2005. *Monitoring Manual for Grassland, Shrubland and Savanna Ecosystems*, 236. Las Cruces, NM, USA: USDA-ARS Jornada Experimental Range.

Hill, J., P. Hostert, G. Tsiourlis, P. Kasapidis, T. Udelhoven, and C. Diemer. 1998. "Monitoring 20 Years of Increased Grazing Impact on the Greek Island of Crete with Earth Observation Satellites." *Journal of Arid Environments* 39: 165–178. doi:10.1006/jare.1998.0392.

Hoekstra, J. M., T. M. Boucher, T. H. Ricketts, and C. Roberts. 2005. "Confronting a Biome Crisis: Global Disparities of Habitat Loss and Protection." *Ecology Letters* 8: 23–29. doi:10.1111/j.1461-0248.2004.00686.x.

Holechek, J. 1988. "An Approach for Setting the Stocking Rate." *Rangelands* 10: 10–14.

Holechek, J., H. Gomez, F. Molinar, and D. Galt. 1999. "Grazing Studies: What We've Learned." *Rangelands* 21 (2): 12–16.

Hudak, A. T., N. L. Crookston, J. S. Evans, M. J. Falkowski, A. M. S. Smith, P. E. Gessler, and P. Morgan. 2006. "Regression Modeling and Mapping of Coniferous Forest Basal Area and Tree Density from Discrete-return Lidar and Multispectral Satellite Data." *Canadian Journal of Remote Sensing* 32 (2): 126–138. doi:10.5589/m06-007.

Huete, A. R. 1988. "A Soil-Adjusted Vegetation Index (SAVI)." *Remote Sensing of Environment* 25: 295–309. doi:10.1016/0034-4257(88)90106-X.

Hunt, E. R., J. H. Everitt, J. C. Ritchie, M. S. Moran, D. T. Booth, G. L. Anderson, P. E. Clark, et al. 2003. "Applications and Research Using Remote Sensing for Rangeland Management." *Photogrammetric Engineering & Remote Sensing* 69 (6): 675–693. doi:10.14358/PERS.69.6.675.

Ikeda, H., K. Okamoto, and M. Fukuhara. 1999. "Estimation of Aboveground Grassland Phytomass with a Growth Model Using Landsat TM and Climate Data." *International Journal of Remote Sensing* 20 (11): 2283–2294. doi:10.1080/014311699212254.

Johnson, T. N., P. L. Kennedy, T. DelCurto, and R. V. Taylor. 2011. "Bird Community Responses to Cattle Stocking Rates in a Pacific Northwest Bunchgrass Prairie." *Agriculture, Ecosystems & Environment* 144: 338–346. doi:10.1016/j.agee.2011.10.003.

Johnson, T. N., P. L. Kennedy, and M. A. Etterson. 2012. "Nest Success and Cause-Specific Nest Failure of Grassland Passerines Breeding in Prairie Grazed by Livestock." *The Journal of Wildlife Management* 76 (8): 1607–1616. doi:10.1002/jwmg.437.

Jordan, C. F. 1969. "Derivation of Leaf-Area Index from Quality of Light on the Forest Floor." *Ecology* 50 (4): 663–666. doi:10.2307/1936256.

Kagan, J., J. Ohmann, M. Gregory, C. Tobalske, J. Hak, and J. Fried. 2006. *Final Report on Land Cover Mapping Methods: Map Zones 8 and 9*. PNW ReGAP. Portland: Institute for Natural Resouces, Oregon State University.

Kauth, R. J., and G. S. Thomas. 1976, "The Tasselled Cap – A Graphic Description of the Spectral-Temporal Development of Agricultural Crops as Seen by LANDSAT." Proceedings of the Symposium on Machine Processing of Remotely Sensed Data. Purdue University, West LaFayett, IN, June 29–July 1.

Kawamura, K., T. Akiyama, H. Yokota, M. Tsutsumi, T. Yasuda, O. Watanabe, and S. Wang. 2005. "Quantifying Grazing Intensities Using Geographic Information Systems and Satellite Remote Sensing in the Xilingol Steppe Region, Inner Mongolia, China." *Agriculture, Ecosystems & Environment* 107: 83–93. doi:10.1016/j.agee.2004.09.008.

Key, C. H. 2006. "Ecological and Sampling Constraints on Defining Landscape Fire Severity." *Fire Ecology* 2 (2): 34–59. doi:10.4996/fireecology.

Key, C. H., and N. C. Benson. 2006. *Landscape Assessment (LA) Sampling and Analysis Methods*, 1–55. Ogden, UT: U.S.D.A. Forest Service, Rocky Mountain Research Station.

Kimoto, C., S. J. DeBano, R. W. Thorp, S. Rao, and W. P. Stephen. 2012. "Investigating Temporal Patterns of a Native Bee Community in a Remnant North American Bunchgrass Prairie Using Blue Vane Traps." *Journal of Insect Science* 12 (108): 1–23. doi:10.1673/031.012.10801.

Knipling, E. 1970. "Physical and Physiological Basis for the Reflectance of Visible and Near-Infrared Radiation from Vegetation." *Remote Sensing of Environment* 1 (3): 155–159. doi:10.1016/S0034-4257(70)80021-9.

Kurtz, D. B., J. Schellberg, and M. Braun. 2010. "Ground and Satellite Based Assessment of Rangeland Management in Sub-Tropical Argentina." *Applied Geography* 30 (2): 210–220. doi:10.1016/j.apgeog.2009.01.006.

Lilliefors, H. 1967. "On the Kolmogorov-Smirnov Test for Normality with Mean and Variance Unknown." *Journal of the American Statistical Association* 62: 399–402. doi:10.1080/01621459.1967.10482916.

Lind, M., K. Rasmussen, H. Adriansen, and A. Ka. 2003. "Estimating Vegetative Productivity Gradients Around Watering Points in the Rangelands of Northern Senegal Based on NOAA AVHRR Data." *Danish Journal of Geography* 103: 1–16. doi:10.1080/00167223.2003.10649475.

Marsett, R. C., J. Qi, P. Heilman, S. H. Biedenbender, M. C. Watson, S. Amer, M. Weltz, D. Goodrich, and R. Marsett. 2006. "Remote Sensing for Grassland Management in the Arid Southwest." *Rangeland Ecology & Management* 59 (5): 530–540. doi:10.2111/05-201R.1.

Masek, J. G., E. F. Vermote, N. E. Saleous, R. Wolfe, F. G. Hall, K. F. Huemmrich, F. Gao, J. Kutler, and T. Lim. 2006. "A Landsat Surface Reflectance Dataset for North America, 1990–2000." *IEEE Geoscience and Remote Sensing Letters* 3 (1): 68–72. doi:10.1109/LGRS.2005.857030.

McLean, A., and E. W. Tisdale. 1972. "Recovery Rate of Depleted Range Sites Under Protection from Grazing." *Journal of Range Management* 25: 178–184. doi:10.2307/3897051.

Merzlyak, M. N., A. A. Gitelson, O. B. Chivkunova, and V. Y. Rakitin. 1999. "Non-Destructive Optical Detection of Pigment Changes During Leaf Senescence and Fruit Ripening." *Physiologia Plantarum* 106: 135–141. doi:10.1034/j.1399-3054.1999.106119.x.

Milchunas, D. G., and W. K. Lauenroth. 1993. "Quantitative Effects of Grazing on Vegetation and Soils Over a Global Range of Environments." *Ecological Monographs* 63 (4): 327–366. doi:10.2307/2937150.

Munyati, C., and D. Makgale. 2009. “Multitemporal Landsat TM Imagery Analysis for Mapping and Quantifying Degraded Rangeland in the Bahurutshe Communal Grazing Lands, South Africa.” *International Journal of Remote Sensing* 30 (14): 3649–3668. doi:10.1080/01431160802592534.

Numata, I., D. A. Roberts, O. A. Chadwick, J. Schimel, F. R. Sampaio, F. C. Leonidas, and J. V. Soares. 2007. “Characterization of Pasture Biophysical Properties and the Impact of Grazing Intensity Using Remotely Sensed Data.” *Remote Sensing of Environment* 109 (3): 314–327. doi:10.1016/j.rse.2007.01.013.

Oak Ridge National Laboratory Distributed Active Archive Center (ORNL DAAC). 2012. MODIS subsetted land products, Collection 5. Accessed October 16, 2012 Oak Ridge, TN: ORNL DAAC. http://daac.ornl.gov/ MODIS/modis.html. Subset obtained for MOD13Q1 product at 45.46590N, 117.15820W, time period: 2000-02-18 to 2012-08-28, and subset size: 130.25 x 80.25 km.

Parsons, C. T., P. A. Momont, T. Delcurto, M. McInnis, and M. L. Porath. 2003. “Cattle Distribution Patterns and Vegetation Use in Mountain Riparian Areas.” *Journal Of Range Management* 56 (4): 334–341. doi:10.2307/4004036.

Paudel, K. P., and P. Andersen. 2010. “Assessing Rangeland Degradation Using Multi Temporal Satellite Images and Grazing Pressure Surface Model in Upper Mustang, Trans Himalaya, Nepal.” *Remote Sensing of Environment* 114 (8): 1845–1855. doi:10.1016/j.rse.2010.03.011.

Pickup, G., G. N. Bastin, and V. H. Chewings. 1994. “Remote-Sensing-Based Condition Assessment for Nonequilibrium Rangelands Under Large-Scale Commercial Grazing.” *Ecological Applications* 4 (3): 497–517. doi:10.2307/1941952.

Pickup, G., G. N. Bastin, and V. H. Chewings. 1998. “Identifying Trends in Land Degradation in Non-Equilibrium Rangelands.” *Journal of Applied Ecology* 35: 365–377. doi:10.1046/j.1365-2664.1998.00319.x.

Purevdorj, T., R. Tateishi, T. Ishiyama, and Y. Honda. 1998. “Relationships Between Percent Vegetation Cover and Vegetation Indices.” *International Journal of Remote Sensing* 19 (18): 3519–3535. doi:10.1080/014311698213795.

Robel, R. J., J. N. Briggs, A. D. Dayton, and L. C. Hulbert. 1970. “Relationships Between Visual Obstruction Measurements and Weight of Grassland Vegetation.” *Journal Of Range Management* 23 (4): 295–297. doi:10.2307/3896225.

Roberts, D. A., M. O. Smith, and J. B. Adams. 1993. “Green Vegetation, Nonphotosynthetic Vegetation, and Soils in AVIRIS Data.” *Remote Sensing of Environment* 44 (2–3): 255–269. doi:10.1016/0034-4257(93)90020-X.

Röder, A., T. Udelhoven, J. Hill, G. Del Barrio, and G. Tsiourlis. 2008. “Trend Analysis of Landsat-TM and -ETM+ Imagery to Monitor Grazing Impact in a Rangeland Ecosystem in Northern Greece.” *Remote Sensing of Environment* 112 (6): 2863–2875. doi:10.1016/j.rse.2008.01.018.

Roujean, J., and F. Breon. 1995. “Estimating PAR Absorbed by Vegetation from Bidirectional Reflectance Measurements.” *Remote Sensing of Environment* 51 (3): 375–384. doi:10.1016/0034-4257(94)00114-3.

Rouse, J. W., R. H. Haas, J. A. Schell, and D. W. Deering. 1973. “Monitoring Vegetation Systems in the Great Plains with ERTS.” In *Proceedings of the third Earth Resources Technology Satellite-1 Symposium*, 309–317. Washington, DC: NASA.

Schino, G., F. Borfecchia, L. De Cecco, C. Dibari, M. Iannetta, S. Martini, and F. Pedrotti. 2003. “Satellite Estimate of Grass Biomass in a Mountainous Range in Central Italy.” *Agroforestry Systems* 59: 157–162. doi:10.1023/A:1026308928874.

Skovlin, J. M., R. W. Harris, G. S. Strickler, and G. A. Garrison. 1976. *Effects of Cattle Grazing Methods on Ponderosa Pine-Bunchgrass Range in the Pacific Northwest*. Technical Bulletin No. 1531. Portland, OR: U.S.D.A. Forest Service, Pacific Northwest Research Station.

Smith, A. M. S., C. A. Kolden, W. T. Tinkham, A. F. Talhelm, J. D. Marshall, A. T. Hudak, L. Boschetti, M. J. Falkowski, J. A. Greenberg, J. W. Anderson, A. Kliskey, L. Alessa, R. F. Keefe, and J. R. Gosz. 2014. “Remote Sensing the Vulnerability of Vegetation in Natural Terrestrial Ecosystems.” *Remote Sensing of Environment* 154: 322–337. doi:10.1016/j.rse.2014.03.038.

Sugiura, N. 1978. “Further Analysts of the Data by Akaike’s Information Criterion and the Finite Corrections.” *Communications in Statistics - Theory and Methods* 7: 13–26. doi:10.1080/03610927808827599.

Svoray, T., A. Perevolotsky, and P. M. Atkinson. 2013. “Ecological Sustainability in Rangelands: The Contribution of Remote Sensing.” *International Journal of Remote Sensing* 34 (17): 6216–6242. doi:10.1080/01431161.2013.793867.
Todd, S., R. Hoffer, and D. Milchunas. 1998. “Biomass Estimation on Grazed and Ungrazed Rangelands Using Spectral Indices.” *International Journal of Remote Sensing* 19 (3): 427–438. doi:10.1080/014311698216071.
Tsalyuk, M., M. Kelly, K. Koy, W. M. Getz, and H. S. Butterfield. 2015. “Monitoring the Impact of Grazing on Rangeland Conservation Easements Using MODIS Vegetation Indices.” *Rangeland Ecology & Management* 68 (2): 173–185. doi:10.1016/j.rama.2015.01.006.
Tucker, C. J. 1979. “Red and Photographic Infrared Linear Combinations for Monitoring Vegetation.” *Remote Sensing of Environment* 8: 127–150. doi:10.1016/0034-4257(79)90013-0.
Tucker, C. J. 1980. “Remote Sensing of Leaf Water Content in the Near Infrared.” *Remote Sensing of Environment* 10 (1): 23–32. doi:10.1016/0034-4257(80)90096-6.
Tueller, P. T. 1989. “Remote Sensing Technology for Rangeland Management Applications.” *Journal of Range Management* 42 (6): 442–453. doi:10.2307/3899227.
Vescovo, L., and D. Gianelle. 2008. “Using the MIR Bands in Vegetation Indices for the Estimation of Grassland Biophysical Parameters From Satellite Remote Sensing in the Alps Region of Trentino (Italy).” *Advances in Space Research* 41 (11): 1764–1772. doi:10.1016/j.asr.2007.07.043.
Washington-Allen, R. A., N. E. West, R. D. Ramsey, and R. A. Efroymson. 2006. “A Protocol for Retrospective Remote Sensing–Based Ecological Monitoring of Rangelands.” *Rangeland Ecology & Management* 59 (1): 19–29. doi:10.2111/04-116R2.1.
West, N. E. 2003. “History of Rangeland Monitoring in the U.S.A.” *Arid Land Research and Management* 17 (4): 495–545. doi:10.1080/713936110.
Wylie, B. K., D. J. Meyer, L. L. Tieszen, and S. Mannel. 2002. “Satellite Mapping of Surface Biophysical Parameters at the Biome Scale Over the North American Grasslands: A Case Study.” *Remote Sensing of Environment* 79 (2–3): 266–278. doi:10.1016/S0034-4257(01)00278-4.
Xu, D., and X. Guo. 2015. “Evaluating the Impacts of Nearly 30 Years of Conservation on Grassland Ecosystem Using Landsat TM Images.” *Grassland Science*. doi:10.1111/grs.12098.
Yang, X., and X. Guo. 2011. “Investigating Vegetation Biophysical and Spectral Parameters for Detecting Light to Moderate Grazing Effects: A Case Study in Mixed Grass Prairie.” *Central European Journal of Geosciences* 3 (3): 336–348. doi:10.2478/s13533-011-0032-4.
Yang, X., X. Guo, and M. Fitzsimmons. 2012. “Assessing Light to Moderate Grazing Effects on Grassland Production Using Satellite Imagery.” *International Journal of Remote Sensing* 33 (16): 5087–5104. doi:10.1080/01431161.2012.657372.
Zhang, C., and X. Guo. 2008. “Monitoring Northern Mixed Prairie Health Using Broadband Satellite Imagery.” *International Journal of Remote Sensing* 29 (8): 2257–2271. doi:10.1080/01431160701408378.